The 15d-PGJ$_2$ hydrogel ameliorates atopic dermatitis through suppression of the immune response

MARCELO H. NAPIMOGA[1], JULIANA T. CLEMENTE-NAPIMOGA[1], NINA M. MACHABANSKI[1],
MARIA EDUARDA A. JULIANI[1], PEDRO HENRIQUE B. C. ACRAS[1], CRISTINA G. MACEDO[1],
HENRIQUE B. ABDALLA[2], ANTÔNIO JOSÉ DE PINHO Jr[1], ANDRESA B. SOARES[3],
MARCELO SPERANDIO[3] and DANIELE R. DE ARAÚJO[4]

[1]Laboratory of Immunology and Molecular Biology, São Leopoldo Mandic Institute and Research Center, Campinas,
São Paulo 13045-755; [2]Laboratory of Orofacial Pain, Department of Physiology, Piracicaba Dental School,
State University of Campinas, Piracicaba, São Paulo 13414-903; [3]Department of Oral Pathology,
São Leopoldo Mandic Institute and Research Center, Campinas, São Paulo 13045-755;
[4]Center of Human and Natural Sciences, Federal University of ABC, Santo André, São Paulo 09210-580, Brazil

Abstract. The present study examined the efficacy of the topical 15d-PGJ$_2$-poloxamer 407 hydrogel in an atopic dermatitis (AD) animal model. The 15d-PGJ$_2$ hydrogel was prepared and characterized. The examined rats possessed AD-Like cutaneous lesions, which were induced using 2,4-dinitrochlorobenzene, the rats were then treated with a hydrogel vehicle, 15d-PGJ$_2$ hydrogel or tacrolimus for 14 days. The rats were sacrificed and blood samples were collected to quantify the IgE levels. Subsequently, skin biopsies were stained with toluidine blue to identify mast cells and immunohistochemistry was performed for ROR-γt and TNF-α. Histological analyses demonstrated that 15d-PGJ$_2$ hydrogel significantly decreased mast cell infiltration (P<0.05) when compared with the AD-group. Tacrolimus at 0.1% exhibited decreased mast cell infiltration; however, this difference was not statistically significant from the AD-group. Topical 15d-PGJ$_2$ hydrogel and Tacrolimus 0.1% significantly reduced the serum levels of IgE (P<0.05) compared with the AD-group. Immunohistochemistry revealed a significant decrease in ROR-γt and TNF-α positive cell expression (P<0.05) in the 15d-PGJ$_2$ hydrogel group compared with the AD-group. In summary, topical administration of 15d-PGJ$_2$ hydrogel had a beneficial effect on AD symptoms, suggesting that this formulation may be a useful strategy for the treatment of AD.

Correspondence to: Dr Marcelo H. Napimoga, Laboratory of Immunology and Molecular Biology, São Leopoldo Mandic Institute and Research Center, 13 R. José Rocha Junqueira, Campinas, São Paulo 13045-755, Brazil
E-mail: marcelo.napimoga@gmail.com

Introduction

Atopic dermatitis (AD) is a highly pruritic cutaneous disease from an inflammatory background that affects up to 10% of adults and 25% of children (1). The skin of AD-sufferers may feature significantly disruption of the epithelial barrier, exacerbated responsiveness to allergens and defective innate immune response to pathogens (2). According to guidelines from the American Academy of Dermatology, treatment should be commenced using mild to moderate-potency topical corticosteroids when emollients and careful skin care are not able to keep AD under control. Should such an approach fail, then calcineurin inhibitors ought to be considered. Calcineurin inhibition reduces transcription factors that regulate cell division, which in will turn exert an anti-inflammatory effect by selectively preventing T-cell activation. Prolongued use of topical corticosteroids is often associated with epithelial and skin atrophy (3) and may occasionally result in systemic adverse effects, e.g., hypothalamic-pituitary-adrenal suppression, particularly in children (4). Undesirable long-term risks associated with calcineurin inhibitors include lymphoma and cutaneous carcinomas in animal studies (5).

The largest meta-analysis to date comparing the efficacy between corticosteroids and calcineurin inhibitors on 6.954 children and adults with moderate to severe AD concluded that calcineurin inhibitors and corticosteroids are just as effective for managing AD, though the superiority of the former over corticosteroid is yet to be demonstrated to justify routine use (6). Calcineurin inhibitors are expensive and show a greater range of adverse events, such as skin burns and pruritus. There is therefore no consensus as to whether calcineurin inhibitors would represent a superior option in the management of AD. Since the range of drug-based options to treat AD is limited, intense research is underway to develop new pharmacological strategies to tackle AD.

Prostaglandins (PG) are the product of sequential COXs-mediated reactions, which will eventually undergo spontaneous dehydration to PGJ$_2$ *in vitro* and be further enhanced

by albumin-induced catalysis, generating several other derivatives, including 15-deoxy-$^{\Delta 12,14}$-PGJ$_2$ (15d-PGJ$_2$) (7). Similarly to other PGs, 15d-PGJ$_2$ can be actively transported into cells to promptly bind nuclear receptors and modify intracellular signaling factors, thanks to a highly reactive cyclopentenone ring (8). It has been demonstrated that 15d-PGJ$_2$ may be the basis for promising strategies to tackle a variety of inflammatory diseases (9,10). AD is also characterized by mast cell migration into the epidermis to release paracrine mediators, including PGD$_2$, which in aqueous media, will spontaneously dehydrate to yield biologically active cyclopentenone PGs, such as 15d-PGJ$_2$ (11).

Considering the anti-inflammatory potential of 15d-PGJ$_2$, the aim of this study was to test the effectiveness of topical thermoreversible 15d-PGJ$_2$-poloxamer (PL) 407 hydrogel formulation in the 2,4-dinitrochlorobenzene (DNCB)-induced AD animal model.

Materials and methods

Preparation and physico-chemical characterization of 15d-PGJ$_2$ hydrogel. PL 407 hydrogels at 30% w/w were dispersed in deionized water at 4˚C by magnetic stirring (150 rpm) for 12 h until complete dissolution. 15d-PGJ$_2$ was then solubilized in dimethyl sulfoxide (DMSO) and dispersed into the hydrogel at 15 ng/μl. The final DMSO concentration into the hydrogels was 0.015%, which is sufficiently low to avoid skin toxicity.

The 15d-PGJ$_2$-micelle interaction and micellar self-assembly were investigated using dynamic light scattering [(DLS; Nanoseries Zetasizer ZS-Malvern® particle analyzer (Malvern Instruments, Ltd., Malvern, UK)] for determining the micellar hydrodynamic diameter and mean distribution size. For samples preparation, PL or PL-PGJ$_2$ systems (3% w/v) were filtered across a polycarbonate membrane (pore 0.22 μm) and measurements acquired at least three times for sample at a fixed 173˚ angle, at 25˚C to 37˚C.

Drug loading (DL, %) and entrapment efficiency (EE, %) parameters were determined for 3% PL micellar formulation. Aliquots (100 μl) were diluted in 0.02 M monobasic sodium phosphate pH 3.5/acetonitrile (60/40% v/v) solution and analyzed by HPLC method. DL, % (Eq. 1) and EE, % (Eq. 2) were determined as follow:

$$\text{(Eq.1) DL (\%)}=(C_{PGJ2} \text{ in micellar phase}/C_{PL} \text{ in micellar sample}) \times 100$$
$$\text{(Eq. 2) EE (\%)}=(C_{PGJ2} \text{ in micellar phase}/C_{total}) \times 100$$

where C_{PGJ2} is 15d-PGJ$_2$ concentration, C_{PL} is PL concentration, and C_{total} is the total PGJ$_2$ concentration into the samples.

Differential Scanning Calorimetry (DSC) was performed to determine temperature and enthalpy relative to micellization. The hydrogels (30 mg) were placed in sealed aluminum receptacles and underwent three heating-cooling cycles (0 to 50˚C) at 5˚C/min in a DSC equipment (Q-200; TA Instruments, New Castle, DE, USA). An empty receptacle was used as negative control. All thermograms were described as heat flux (cal/g) against temperature (˚C).

The sol-gel transition temperature (Tsol-gel) and gelation kinetics were determined by an oscillatory rheometer

(Kinexus Lab., Malvern Instruments, Ltd.) with a cone-plate geometry, under a temperature range from 10 to 50˚C and frequency at 1 Hz. From the results, parameters related to the elastic (G'), viscous modulus (G'') and viscosity (η) were obtained and data analyzed by rSpace for Kinexus® software.

For investigating the 15d-PGJ$_2$ release mechanisms from PL hydrogel, *in vitro* assays were carried out using a vertical two-compartment diffusion model Franz-type cells (1.76 cm^2 area, Microette Plus®, Hanson Research, Chatsworth, CA, USA). An artificial membrane (cellulose acetate sheets, MWCO 1000 Da, Spectrum Lab) was used as a barrier for separating the two compartments. The donor compartment was filled with 250 μl of 15d-PGJ$_2$ (in ultrapure water) or PL404-PGJ$_2$. 15d-PGJ$_2$ final concentration of 3.75 μg/250 μl for both formulations. Receptor compartment was filled with 7.0 ml of 5 mM Hepes, 154 mM NaCl buffer (pH 7.4, at 37˚C) and maintained under magnetic stirring (350 rpm). Aliquots of 1.0 ml were withdrawn from the receptor compartment at intervals from 0.5 to 24 h. Samples were analyzed by HPLC. Data were expressed as 15d-PGJ$_2$ released percentage against time (h).

Release profiles were then analyzed according to Zero-order (Eq. 3), Higuchi (Eq. 4) and Hixson-Crowell (Eq. 5) models, as described below:

$$Qt=Q_0 + K_0 \, t \text{ (Eq. 3)}$$

where Qt is the cumulative amount of drug released at time t, Q0 is the initial amount of drug, K_0 is the zero-order release constant, and t is time.

$$Qt=K_H \, t^{1/2} \text{ (Eq. 4)}$$

where the rate of drug release is linear as a function of square root of time and the drug is the only component that diffuses through the medium, which the release mechanism is a diffusion process dependent on Fick law. K_H is the release coefficient, and Qt is the drug released amount.

$$Q_0^{1/3}-Q_t^{1/3}=K_{HC} \, t \text{ (Eq. 5)}$$

Q_0 is the initial amount of drug, Q_t is the cumulative amount of drug released, K_{HC} is the release constant and t is time.

HPLC method for 15d-PGJ$_2$ quantification. The 15d-PGJ$_2$ quantification was performed by High Performance Liquid Chromatography (Ultimate 3000 with Chromeleon 7.2 software; Dionex Corporation, Sunnyvale, CA, USA) system composed of quaternary pump, DAD detector and C18 column (150x4.6 mm, 5 μm-Phenomenex). Samples were detected at 216 nm, 0.6 ml/min flow rate (25˚C) and mobile phase composed of 0.02 M monobasic sodium phosphate pH 3.5/acetonitrile (60/40 v/v). Drug retention time was 2.8 min. A calibration curve was obtained from standard solutions (2.5, 5, 50, 250 and 300 ng/ml). The detection (LOD) and quantification (LOQ) limits values were 0.063 and 0.189 ng/ml, respectively, obtained from the previously determined equation (y=0.8378 x + 3.339, R^2=0.989).

Animals. This study was performed on male Wistar rats weighing 200 to 300 g (n=5/per group) and kept in cages

(5 per cage) in a temperature-controlled room (23±1˚C), 12:12 light cycle, with water and food *ad libitum*. All animals were obtained from the Multidisciplinary Center for Biological Investigation on Laboratory Animal Science (CEMIB-UNICAMP) and the experimentation was approved by the Committee on Animal Research of the University of Campinas (approval no. 4088-1), which followed the guidelines by the Brazilian National Council for Control of Animal Experimentation (CONCEA).

Inducing AD-Like Lesions and 15d-PGJ$_2$ hydrogel treatment. Induction of AD-like lesions was adapted from previously published guidelines (12). The DNCB is an aromatic hydrocarbon that when directly apply in the skin induce an inflammation. The skin from the dorsum of the rats was shaved to an area of 1x1 cm and painted once with 200 μl of 1% DNCB. Two weeks after sensitization, the target area on the skin was challenged with 200 μl of 0.2% DNCB solution twice weekly for 2 weeks. Subsequently, one of the following treatments was topically applied once daily over 14 days: i) No treatment; ii) vehicle (PL-407, 3 μl); iii) 15d-PGJ$_2$ hydrogel (75 ng/3 μl) or iv) Tacrolimus 0.1% (Tarfic® 0.1%, Tacrolimus Monohydrate; Libbs Pharmaceutics, São Paulo, Brazil). The treatments were maintained at the site of lesion induction. When the experiment was complete, the animals were sacrificed by CO$_2$ inhalation and skin biopsies were harvested. The AD-protocol is summarized in Fig. 1.

Histological analysis. A portion of the skin biopsies were fixed in neutral formalin and paraffin-embedded. Seven-micrometer tissue sections were taken and stained with toluidine blue for mast cell count.

Initial analysis of the toluidine blue sections were performed by four examiners (ABS, NM, MJ, PA) using a multi-headed microscope. Toluidine blue staining was evaluated both qualitatively and quantitatively. Qualitative analysis was performed via cell positivity in all areas of the section. Quantitative analysis of mast cells was performed by positive cell counting within the subepithelial connective tissue over 10 fields per case at magnification, x400 (x40 objective lens, field diameter of 0.44 mm) using a CCD camera on a Nikon Eclipse Ci microscope. The individual who performed the counting was blind to the experimental groups.

Immunohistochemistry. Five-micrometer sections were immune-stained for ROR-γt and TNF-α. following endogenous peroxidase activity quenching in 3% hydrogen peroxide (Dinâmica, Diadema, SP, Brazil). Antigen retrieval (AR) was performed in boiling citrate buffer (pH 6.0). The primary antibody was incubated overnight at 4˚C, followed by EnVision HRP and Envision+ (K1491; Dako; Agilent Technologies, Inc., Santa Clara, CA, USA) at 37˚C for one hour. The sections were then stained with 3,3'-diaminobenzidine tetrahydrochloride (DAB, Dako; Agilent Technologies, Inc.) for five min at 37˚C and counter-stained with hematoxylin.

ROR-γt and TNF-α expression was evaluated by inflammatory positive cell counting within the subepithelial connective tissue over 10 fields per case at magnification, x400 (x40 objective lens, field diameter of 0.44 mm) using a CCD camera on a Nikon Eclipse Ci microscope. Epithelial cells were not taken into account for ROR-γt and TNF-α expression. The individual who performed the counting was blind to the experimental groups.

Blood sample collection and IgE quantification. Whole blood was collected by cardiac puncture to quantify IgE levels following 15d-PGJ$_2$ hydrogel administration. The blood samples were stored in EDTA Vacutainer tubes containing EDTA (BD Biosciences, Franklin Lakes, NJ, USA) and blood plasma was then isolated. IgE measurements were obtained using ELISA following the manufacturer's instructions (BD Biosciences) via optical density (O.D.) measured at 450 nm and the readings were expressed as pg/ml, according to the standard.

Statistical analysis. To determine if there were significant differences ($P<0.05$) among groups, the data were analyzed using one-way analysis of variance (ANOVA) with post hoc contrasts using the Tukey's test. Data are presented in figures as mean ± standard deviation (SD). All statistical calculations were performed on GraphPad Prism 6® (GraphPad Software, Inc., La Jolla, CA, USA).

Results

Physico-chemical characterization of PL 407 micelles and hydrogel. The hydrodynamic diameter was the parameter used for evaluating the PL 407 micelles formation in the presence or absence of 15d-PGJ$_2$. In general, there were no overall significant changes on micellar hydrodynamic diameter for PL407 systems after 15d-PGJ$_2$ incorporation. Micellar diameters of ~60 nm (average distribution of 88.1±0.7%) and ~5 nm (12.1±0.2%) were observed at 25˚C, while at 37˚C, micellar dimensions were reduced to ~30 nm with 99.6±0.7% and polydispersion values of ~0.25, showing the influence of temperature variation on micellar self-assembly, even in the presence of 15d-PGJ$_2$. For DL % and EE % parameters were obtained values of 44.1±0.2 and 98.0±0.3%, respectively, indicating that PL407 micelles are able to carry high amounts of 15d-PGJ$_2$.

Calorimetric analysis (Table I) showed that micelles formation is an endothermic process (enthalpy values greater than zero), with micellization temperature (Tm) at 17.8 and 15.2˚C, before and after 15d-PGJ$_2$ incorporation. Even slightly different Tm was observed for 15d-PGJ$_2$-PL407, this system presented high enthalpy variation ($\Delta H°=0.31$ cal/g) than that observed for PL407 isolated system ($\Delta H°=0.21$ cal/g).

For PL-based formulations, the rheological behavior provides essential information to study the hydrogel formation and the influence of incorporated molecules into its structure. For this reason, rheological parameters such as elastic (G') and viscous (G'') moduli, viscosity (η) and Tsol-gel (when the most pronounced viscosity variation is observed) were determined before and after 15d-PGJ$_2$ insertion (Table I). Fig. 2 presents the rheograms for PL407 and PL407-15d-PGJ$_2$ under temperature variation. The incorporation of 15d-PGJ$_2$ did not, significantly, shift the Tsol-gel, but evoked pronounced changes on elastic modulus (G') reaching values ~10 times higher than that observed for G''.

Table I. Hydrodynamic diameter, size distribution, themodynamic and rheological parameters for PGJ$_2$-loaded PL407 hydrogels.

	Hydrodynamic diameter (nm)		Average distribution (%)		Tm (°C)	ΔH (kJ.mol^{-1})	G' (.10^{4}Pa)	G'' (.10^{4}Pa)	G'/G''	η (.10^{3}mPa.s)	Tsol-gel (°C)
Formulations	25°C	37°C	25°C	37°C							
PL407	59.7±2.1	31.4±1.7	88.1±2.1 12.1±0.2	94.1±1.6 6.8±0.9	17.8	0.21	1975	648.4	3.04	330900	20.4
PL407-PGJ$_2$	61.2±0.2	29.8±1.3	87.9±1.2 13.1±0.9	99.6±0.8	15.2	0.31	9114	890.5	10.2	1457000	21.8

Tm, micellization temperature; PG, prostaglandin; PL, poloxamer; ΔH, enthalpy variation; G', elastic modulus; G'', viscous modulus; η, viscosity; Tsol-gel, sol-gel transition temperature.
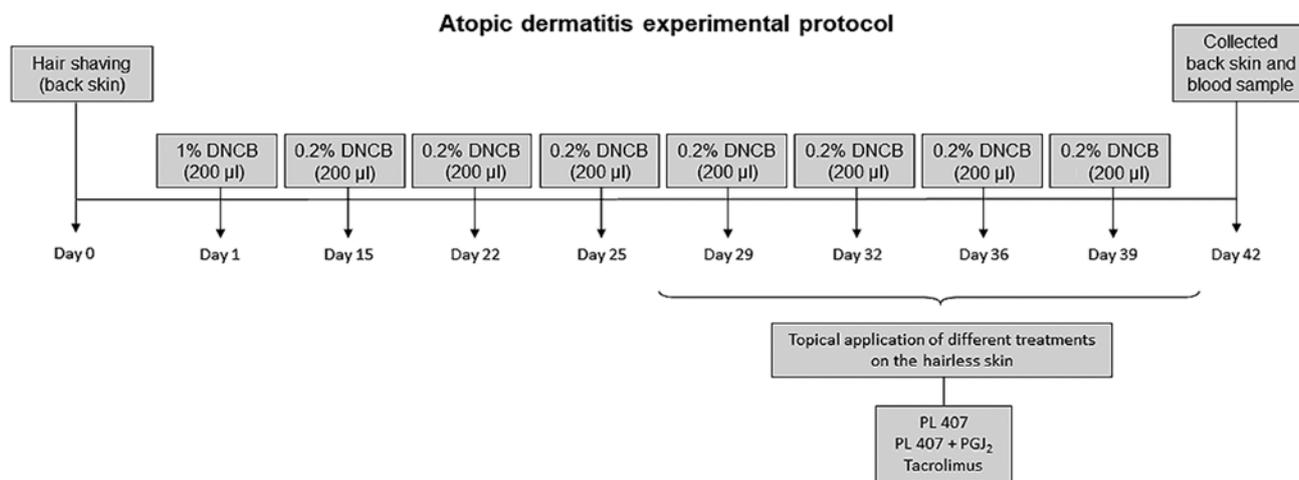

Figure 1. Experimental design. Atopic dermatitis experimental protocol. DNCB, 2,4-dinitrochlorobenzene; PG, prostaglandin; PL, poloxamer.
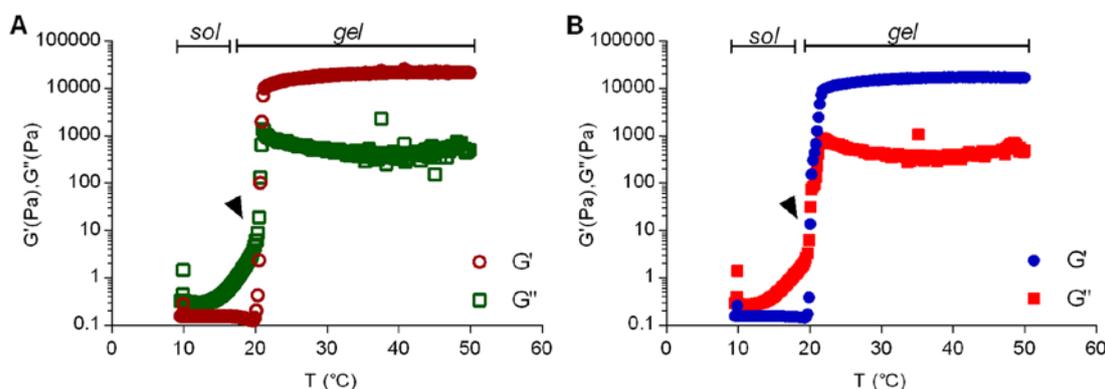

Figure 2. Rheograms presenting temperature curves for (A) PL407 and (B) 15d-PGJ$_2$-PL407 hydrogels. Arrows indicate the Tsol-gel point (sol-gel transition temperature). Tsol-gel, sol-gel transition temperature; PL, poloxamer; G', elastic; G'', viscous modulus.

As demonstrated in Fig. 3 and Table II, the 15d-PGJ$_2$ release profiles and their mathematical models. The 15d-PGJ$_2$ release from aqueous solution reached a maximum release percentage after 4 h. On the other hand, the 15d-PGJ$_2$ released from PL407 hydrogels was sustained and lower drug release percentages were observed until 24 h (62.3%), when compared to 15d-PGJ$_2$ in solution (100%). In general, low release constant (Krel) values were obtained for PL407-PGJ$_2$

(1.4%.h^{-1}; 10.4%.h$^{-1/2}$; 0.15%.h$^{-1/3}$ for Zero Order, Higuchi and Hixson-Crowell models, respectively) in relation to 15d-PGJ$_2$. However, the Hixson-Crowell mathematical model showed the highest correlation coefficient value (R^2=0.97) compared to Zero Order (R^2=0.95) and Higuchi (R^2=0.91).

15d-PGJ$_2$ hydrogel decreases infiltration of mast cells into AD-like skin lesions. To establish whether 15d-PGJ$_2$ hydrogel

Table II. Release constants and determination coefficients obtained for PGJ_2 from PL407 (30% wt) hydrogel.

Formulations	Zero Order		Higuchi		Hixson-Crowell	
	K_0 (%.h^{-1})	R^2	K_H (%.h$^{-1/2}$)	R^2	K_{HC} (%.h$^{-1/3}$)	R^2
PGJ_2	2.4±0.4	0.84	15.0±1.2	0.85	0.46±0.05	0.87
PL407-PGJ_2	1.4±0.9	0.91	10.4±4.4	0.95	0.15±0.01	0.97

K_H, the release coefficient; K_0, zero-order release constant.
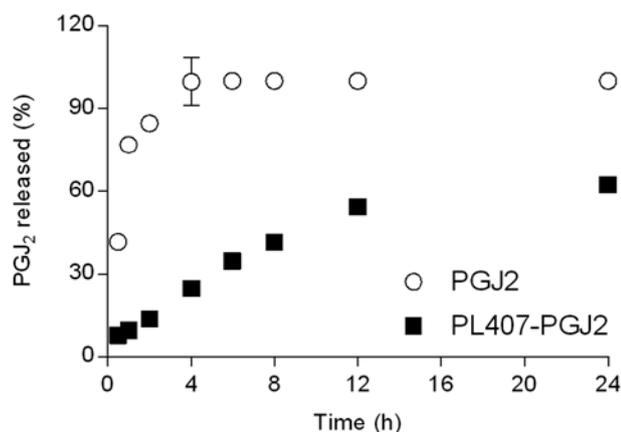
Figure 3. 15d-PGJ_2 release profiles from PL407 (30%) hydrogel (n=3/formulation).

reduces mast cell infiltration into AD-like skin lesions, toluidine blue staining was performed on the skin biopsies following topical administration of 15d-PGJ_2 or vehicle (Fig. 4). Mast cell infiltration was detected in the AD-like group and the AD-like group treated with vehicle (PL-407), where the 15d-PGJ_2 hydrogel significantly decreased ($P<0.05$) such infiltration of mast cells into the skin when compared with AD-like and AD-like + PL-407 (Fig. 5). Moreover, the group treated with Tacrolimus 0.1% also decreased mast cell infiltration, although no statistically significant difference was detected when compared to both untreated groups. The data on mast cell counts is shown in Fig. 5.

Measurement of total plasma IgE level in AD-like skin lesion. High IgE levels are a major feature of AD and those diagnosed with AD often exhibit high levels of total IgE and also allergen-specific IgE. Serum levels of IgE in the AD-like group and AD-like treated with vehicle were significantly higher than that in the disease-free group. The administration of topical 15d-PGJ_2 hydrogel or Tacrolimus 0.1% significantly reduced the serum levels of IgE ($P<0.05$) compared to AD-like groups (Fig. 6).

Effect of 15d-PGJ_2 hydrogel on ROR-γ expression in rat skin tissue. To determine whether 15d-PGJ_2 hydrogel decreases Th17 type lymphocyte, we performed immunohistochemistry to quantify the transcription factor ROR-γt (Fig. 4). We found that topical administration of 15d-PGJ_2 hydrogel significantly decreased the number of immunostained cells compared to the AD-like group ($P<0.05$). No significant difference was observed

between the AD-like group and the Tacrolimus-treated group ($P>0.05$), nor was it observed between the 15d-PGJ_2 hydrogel and the Tacrolimus groups ($P>0.05$). The data are shown in Fig. 7A.

Effect of 15d-PGJ_2 hydrogel on TNF-α expression in rat skin tissue. Immunohistochemistry was performed to verify whether 15d-PGJ_2 hydrogel would reduce TNF-α expression (Fig. 4). The number of immunostained cells in the AD-like group and the AD-like group treated with vehicle significantly increased in comparison to the disease-free specimens ($P<0.05$). Moreover, topical administration of 15d-PGJ_2 hydrogel significantly reduced the TNF-α-positive cell count from the AD-like groups ($P<0.05$). It is important to highlight that no significant difference was detected between the AD-like group and the Tacrolimus-treated group ($P>0.05$). The data are described in Fig. 7B.

Discussion

The prostaglandin known as 15d-PGJ_2 is an endogenous PG that binds to PPAR-γ generated during the resolution phase of inflammation following tissue injury (13) and it has shown a potent anti-inflammatory action when administrated exogenously (10,14,15). Moreover, improved bioavailability and efficiency of such compound has been achieved from different strategies to couple the 15d-PGJ_2 molecule to carrier systems (9,16,17). In this study, we demonstrated that topical administration of 15d-PGJ_2 hydrogel had a beneficial effect on AD symptoms, suggesting a potentially useful role for this formulation in the management of AD.

Considering that micellar dimensions were reduced at physiological temperature, micelles can remain at the site of administration for long periods of time and be small enough (<100 nm) to avoid uptake by the reticuloendothelial system, favoring the therapeutic efficacy of the drug carrier (18). In fact, for PL systems (such as PL 407), reductions on micellar hydrodynamic diameters in response to temperature changes are well-described in the literature. This phenomenon is attributed to the dehydration of PL polyoxypropylene oxide units from micellar core, reducing the micellar dimensions and promoting the formation of a colloidal system with spherical and almost identical micelles (19-21).

PL407 is a relatively hydrophilic PL type with hydrophilic lipophilic balance value of 22, due to differences on its polyethylene oxide (PEO) and polypropylene oxide (PPG) units number. The 1:3 units PEO:PPO relationship characterize its chemical structure making possible the formation of both
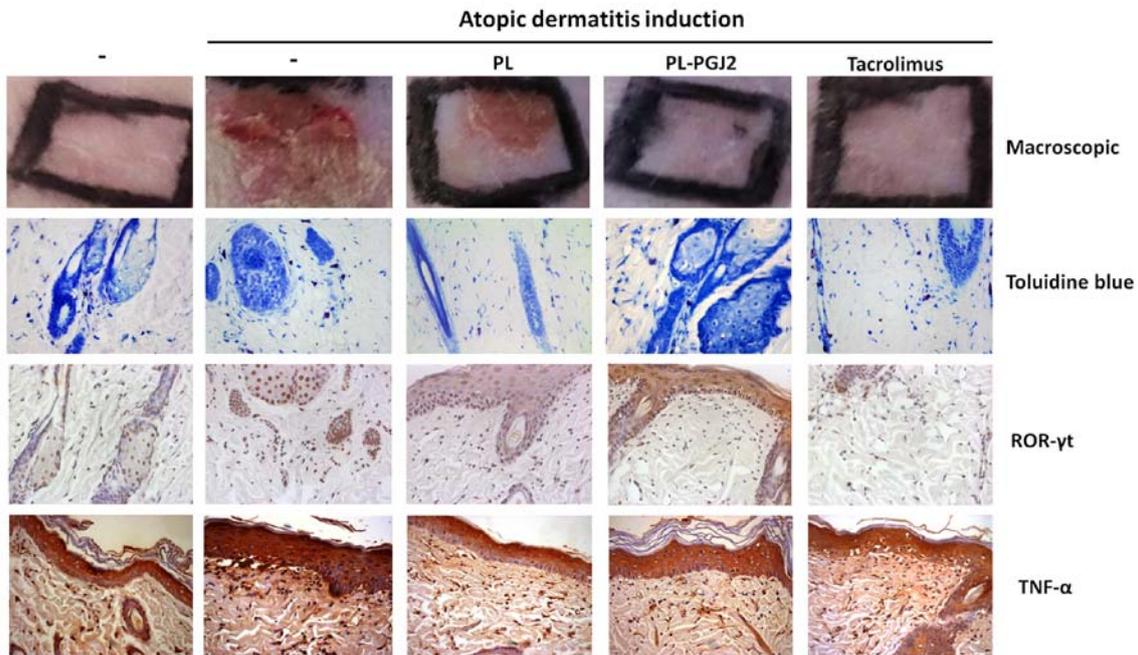
Figure 4. Macroscopic aspect, toluidine blue staining, immunohistochemistry for ROR-γt transcription factor and immunohistochemistry for TNF-α of the DA-induced lesion and AD-treated animals (magnification, x400). AD, atopic dermatitis.
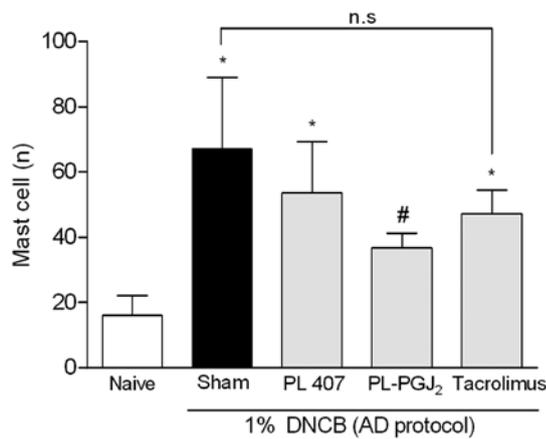

Figure 5. Mast cell count in AD-like skin lesions. The skin sections were stained with toluidine blue for mast cells. Quantitative analysis of mast cells was performed by positive cell counting within the subepithelial connective tissue over 10 fields per case at magnification, x400. The data are presented as mean ± SD of 5 animals per group. The symbol (*) indicates a mast cell counting significantly higher than Naïve group (non AD-group) (P<0.05: ANOVA, Tukey's test). The symbol (#) indicates a mast cell counting significantly lower than AD-group group (P<0.05: ANOVA, Tukey's test). n.s, not significant; AD, atopic dermatitis; SD, standard deviation; ANOVA, one-way analysis of variance; PG, prostaglandin; PL, poloxamer; DNCB, 2,4-dinitrochlorobenzene.
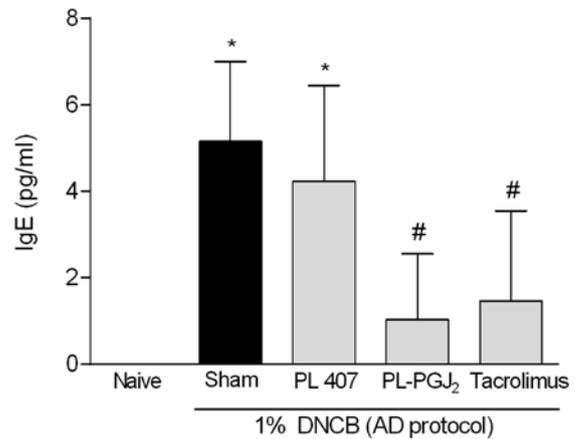
Figure 6. Measurement of plasma IgE level. Total IgE level was determined by ELISA. The data are presented as mean ± SD of 5 animals per group. The symbol (*) indicates an IgE levels significantly higher than Naïve group (non AD-group) (P<0.05: ANOVA, Tukey's test). The symbol (#) indicates an IgE levels significantly lower than AD-group (P<0.05: ANOVA, Tukey's test). n.s, not significant; AD, atopic dermatitis; ANOVA, one-way analysis of variance; DNCB, 2,4-dinitrochlorobenzene; PG, prostaglandin; PL, poloxamer.

micellar hydrophobic core and hydrophilic corona capable of self-organization in a hydrogel supramolecular structure, responding to the presence of different molecules according to their chemical structure (22). Fig. 8 presents the sol-gel transition phenomena from PL unimers to micelles and their self-assembly as hydrogels in response to concentration and temperature, forming a final hydrogel formulation proposed here.

Calorimetry analysis showed no significant shifts regarding to temperature for micelles formation. However, differences were observed for enthalpy variation value after 15d-PGJ₂ incorporation, showing the drug interference on micellar self-assembly possibly due to its insertion into the system, as also described for different hydrophobic molecules (23-25). One of the main advantages of this system is the ability to incorporate hydrophobic molecules. Then, the hydrophobicity of the PL micellar core (due to polypropylene oxide units dehydration) and the 15d-PGJ₂ chemical structure, as a low molecular weight prostanoid derivative (molecular weight of 316.4, $C_{20}H_{28}O_3$), are important features for favoring its incorporation into PL407 micelles, explaining the high 15d-PGJ₂ DL and encapsulation efficiency percentages. Additionally, no changes were observed on thermoreversible
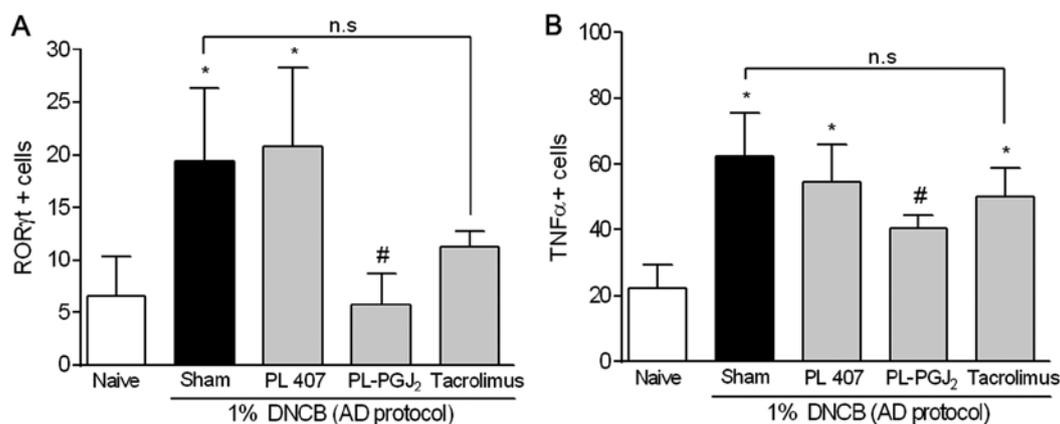
Figure 7. Effect of 15d-PGJ$_2$ hydrogel on the (A) ROR-γ and (B) TNF-α expression in rat skin tissue measured by immunohistochemistry. The data are presented as mean ± SD of 5 animals per group. The symbol (*) indicates a ROR-γ or TNF-α expression significantly higher than Naïve group (non AD-group) ($P<0.05$: ANOVA, Tukey's test). The symbol (#) indicates a ROR-γ or TNF-α expression significantly lower than AD-group ($P<0.05$: ANOVA, Tukey's test). 15d-PGJ$_2$, 15-deoxy-$^{\Delta 12,14}$-PGJ$_2$; PG, prostaglandin; PL, poloxamer; AD, atopic dermatitis; n.s, not significant; DNCB, 2,4-dinitrochlorobenzene; ANOVA, one-way analysis of variance; SD; standard deviation.
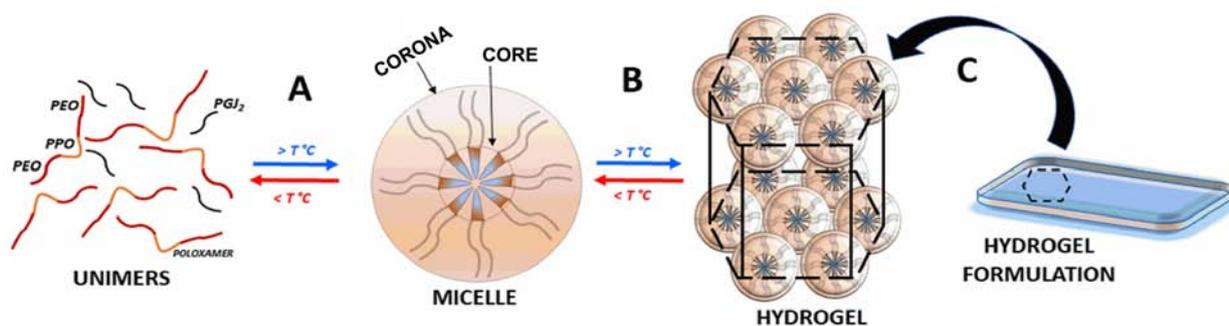

Figure 8. Schematic representation of thermosensitive sol-gel transition phenomenon for poloxamer-based hydrogels. (A) Transition from PL unimers for micelles with PEO and PPO blocks aggregation; (B) micelles self-assembly as hydrogel supramolecular structure; (C) hydrogel formulation containing PGJ$_2$. PG, prostaglandin; PL, poloxamer; PEO, polyethylene oxide; PPO, polypropylene oxide.

properties, indicating the stability of the hydrogel systems after 15d-PGJ$_2$ incorporation. Rheological analysis provided important information regarding the sol-gel process kinetics, showing the formation of a structurally ordered and viscous hydrogel due to the predominance of elastic over viscous properties and increased viscosity values after 15d-PGJ$_2$ incorporation. The 15d-PGJ$_2$-loaded hydrogels showed low release constant value determined by the drug dissolution rate and its permeation during the hydrogel polymeric matrix erosion. This mechanism contributes to the formation of hydrated matrices due to the water penetration across the polymer chains (23,26).

In this study, we presented the development of a topical hydrogel formulation for AD based on 15d-PGJ$_2$-loaded PL407 hydrogel. The *in vitro* assays showed an extended release profile, being possible to predict that low 15d-PGJ$_2$ concentrations could be in contact to the site of application. According to the pharmacological daily scheme proposed here, a hydrogel volume of 3 μl was applied providing a 15d-PGJ$_2$ final concentration of 75 ng in contact to the skin area lesions. Since ~60% of encapsulated 15d-PGJ$_2$ was quantified after 24 h, that concentration was sufficiently released from hydrogels formulation explaining the formulation efficiency in terms of available drug concentration, despite the differences between *in vitro* and *in vivo* studies.

Regarding to molecular mechanism for AD treatment, there are two main concerns: the first is that AD is a chronic disease and long-term topical steroid use may lead to skin atrophy (27) and the second is that calcineurin inhibitors do not affect skin thickness but carry an increased risk of inducing skin cancer (28). We have demonstrated that topical administration of 15d-PGJ$_2$ hydrogel significantly reduced mast cell infiltration into the skin, reinforced by the fact that the outer aspect of the epidermis on the treated animals looked visibly normal (Figs. 4 and 5). A previous study showed that subcutaneous administration of 15d-PGJ$_2$ suppressed Bleomycin-induced skin sclerosis, despite no significant suppression of mast cell infiltration, but significant inhibition of the mast cell activation process (29). Furthermore, 15d-PGJ$_2$ was found to inhibit a series of fibroblast-associated processes, such as TGF-β stimulation of collagen gene expression, transdifferentiation of myofibroblasts (30) as well as the Smad-dependent promoter activity (31). 15d-PGJ$_2$ has also been shown to attenuate the proliferation of keloid cells, inhibit collagen gel contraction as well as to increase cleavage of caspase-3 (32). It has been demonstrated, however, that 15d-PGJ$_2$ and a prostanoid DP2 receptor agonist (13,14-dihydro-15-keto-prostaglandin D2) had no clear effect on the scratching behavior of rodents, thus suggesting that such prostaglandin D2 suppressive effect ought to be mediated by the prostanoid DP1 receptor instead (33).

A previous study demonstrated that 15d-PGJ$_2$ is able to reduce IgE levels and inhibit the proliferation of LPS-induced B cells in an asthma-like model (34) Furthermore, 15d-PGJ$_2$ was able to reduce FcERI expression, thus bypassing IgE binding to cells, which in turn decreased the secretion of important allergic inflammation activators (35). Additionally, previous reports have shown that 15d-PGJ$_2$ can inhibit the IgE-switch in B-cells by suppressing the phosphorylation of STAT-6 (36). Corroborating with this previous findings, we showed that both treatments (15d-PGJ$_2$ hydrogel or Tacrolimus 0.1%) significantly reduced systemic IgE levels when compared to the AD-like group. Beyond that, 15d-PGJ$_2$ hydrogel or Tacrolimus 0.1% groups shown no difference when compared each other.

The role of the Th17 pathway has recently been extensively explored in chronic inflammatory illnesses. While a fundamentally autoimmune role has been associated with activation of the Th17 pathway (37,38), emerging data suggest that IL-17 and Th17 participate in the pathogenesis of AD, where IL-17 expression is upregulated in patients with acute AD lesions (39). Furthermore, Koga *et al* (40) have shown a correlation between circulating Th17 cells and the severity of acute AD. Besides, AD is considered a biphasic inflammation, in which Th2-mediated disease is predominant in the acute phase, switching towards the Th1-Th17 environment in chronic disease (41). Activated immune cells (macrophages and T cells) secrete TNF-α, which may also be produced by mast cells in response to IgE (42). Our data have shown that 15d-PGJ$_2$ hydrogel was able to decrease the Th17 population at the site of AD, whereas Tacrolimus 0.1% failed to do so. This is a highly relevant observation, since IL-17 plays its part in modulating immune dysregulation and affecting the integrity of the skin barrier (43). Furthermore, upregulation of IL-17 *in situ* and circulating interleukin levels in AD reiterates the systemic inflammatory nature of such condition (44). Additionally, a significantly decreased in TNF-α expression was observed in group treated with 15d-PGJ$_2$ hydrogel but not with Tacrolimus 0.1%. This an important finding since it is well-known hat TNF-α is a key accessory mediator of T cell activation in AD.

As 15d-PGJ2 may have multiple effects on animal models of AD, more studies are needed to fully elucidate its role on treating allergic diseases. The PPAR-γ pathway may be one such target, since previous studies have shown that 15d-PGJ$_2$ activation of PPAR-γ has an anti-inflammatory effect in an asthma model, which is yet another atopic condition (45).

The present study clearly shows that 15d-PGJ$_2$ hydrogel was able to suppress the progression of DNBC-induced AD. In addition, IgE levels decreased as well as Th17 and TNF-α positive cells. The emerging of a possible new treatment for AD that could be as effective as the current available with potentially fewer side-effects and a wider spectrum of action in the mechanism of atopic inflammation should be evaluated in a clinical trial. In conclusion, this new formulation of 15d-PGJ$_2$ hydrogel may be a useful strategy in the management of AD.

Acknowledgements

Funding

Availability of data and materials

The datasets used and/or analyzed during the current study are available from the corresponding author on reasonable request.

Authors' contributions

MHN, AJDPJ and DRDA designed the study. CGM and HBA performed the animal model experiments. NMM, MEAJ, PHBCA, ABS and MS acquired the data. MHN, JTCN, ABS, MS and DRDA analyzed and interpreted the data, and drafted the manuscript. All authors critically revised the manuscript, and read and approved the final version of the manuscript.

Ethics approval and consent to participate

All animal experimental procedures and protocols were approved by the Committee on Animal Research of the University of Campinas (approval no. 4088-1) and are in accordance with guidelines of CONCEA.

Patient consent for publication

Not applicable.

Competing interests

The authors declare that they have no competing interests.

References

1. Veiga SP: Epidemiology of atopic dermatitis: A review. Allergy Asthma Proc 33: 227-234, 2012.
2. De Benedetto A, Kubo A and Beck LA: Skin barrier disruption: A requirement for allergen sensitization? J Invest Dermatol 132: 949-963, 2012.
3. Berke R, Singh A and Guralnick M: Atopic dermatitis: An overview. Am Fam Physician 86: 35-42, 2012.
4. Dhar S, Seth J and Parikh D: Systemic side-effects of topical corticosteroids. Indian J Dermatol 59: 460-464, 2014.
5. Margolis DJ, Abuabara K, Hoffstad OJ, Wan J, Raimondo D and Bilker WB: Association between malignancy and topical use of pimecrolimus. JAMA Dermatol 151: 594-599, 2015.
6. Broeders JA, Ahmed Ali U and Fischer G: Systematic review and meta-analysis of randomized clinical trials (RCTs) comparing topical calcineurin inhibitors with topical corticosteroids for atopic dermatitis: A 15-year experience. J Am Acad Dermatol 75: 410-419, 2016.
7. Kikawa Y, Narumiya S, Fukushima M, Wakatsuka H and Hayaishi O: 9-Deoxy-delta 9, delta 12-13,14-dihydroprostaglandin D2, a metabolite of prostaglandin D2 formed in human plasma. Proc Natl Acad Sci USA 81: 1317-1321, 1984.
8. Straus DS and Glass CK: Cyclopentenone prostaglandins: New insights on biological activities and cellular targets. Med Res Rev 21: 185-210, 2001.

9. Napimoga MH, da Silva CA, Carregaro V, Farnesi-de-Assunção TS, Duarte PM, de Melo NF and Fraceto LF: Exogenous administration of 15d-PGJ₂-loaded nanocapsules inhibits bone resorption in a mouse periodontitis model. J Immunol 189: 1043-1052, 2012.

10. Macedo CG, Napimoga MH, Rocha-Neto LM, Abdalla HB and Clemente-Napimoga JT: The role of endogenous opioid peptides in the antinociceptive effect of 15-deoxyΔ12,14-prostaglandinJ2 in the temporomandibular joint. Prostaglandins Leukot Essent Fatty Acids 110: 27-34, 2016.

11. Shibata T, Takahashi K, Matsubara Y, Inuzuka E, Nakashima F, Takahashi N, Kozai D, Mori Y and Uchida K: Identification of a prostaglandin D2 metabolite as a neuritogenesis enhancer targeting the TRPV1 ion channel. Sci Rep 16: 21261, 2016.

12. Kim SR, Choi HS, Seo HS, Ku JM, Hong SH, Yoo HH, Shin YC and Ko SG: Oral administration of herbal mixture extract inhibits 2,4-dinitrochlorobenzene-induced atopic dermatitis in BALB/c mice. Mediators Inflamm 2014: 319438, 2014.

13. Surh YJ, Na HK, Park JM, Lee HN, Kim W, Yoon IS and Kim DD: 15-Deoxy-Δ¹²,¹⁴-prostaglandin JZ, an electrophilic lipid mediator of anti-inflammatory and pro-resolving signaling. Biochem Pharmacol 82: 1335-1351, 2011.

14. Silva Quinteiro M, Henrique Napimoga M, Gomes Macedo C, Furtado Freitas F, Balassini Abdalla H, Bonfante R and Trindade Clemente-Napimoga J: 15-deoxy-Δ12,14-prostaglandin J2 reduces albumin-induced arthritis in temporomandibular joint of rats. Eur J Pharmacol 740: 58-65, 2014.

15. Napimoga MH, Vieira SM, Dal-Secco D, Freitas A, Souto FO, Mestriner FL, Alves-Filho JC, Grespan R, Kawai T, Ferreira SH and Cunha FQ: Peroxisome proliferator-activated receptor-gamma ligand, 15-deoxy-Delta12,14-prostaglandin J2, reduces neutrophil migration via a nitric oxide pathway. J Immunol 180: 609-617, 2008.

16. Clemente-Napimoga JT, Moreira JA, Grillo R, de Melo NF, Fraceto LF and Napimoga MH: 15d-PGJ₂-loaded in nanocapsules enhance the antinociceptive properties into rat temporomandibular hypernociception. Life Sci 90: 944-949, 2012.

17. Alves C, de Melo N, Fraceto L, de Araújo D and Napimoga M: Effects of 15d-PGJZ-loaded poly(D,L-lactide-co-glycolide) nanocapsules on inflammation. Br J Pharmacol 162: 623-632, 2011.

18. Gaumet M, Vargas A, Gurny R and Delie F: Nanoparticles for drug delivery: The need for precision in reporting particle size parameters. Eur J Pharm Biopharm 69: 1-9, 2008.

19. Trong LC, Djabourov M and Ponton A: Mechanisms of micellization and rheology of PEO-PPO-PEO triblock copolymers with various architectures. J Colloid Interface Sci 328: 278-287, 2008.

20. Oshiro A, da Silva DC, de Mello JC, Moraes VW, Cavalcanti LP, Franco MK, Alkschbirs MI, Fraceto LF, Yokaichiya F, Rodrigues T and de Araujo DR: Pluronics f-127/l-81 binary hydrogels as drug-delivery systems: Influence of physicochemical aspects on release kinetics and cytotoxicity. Langmuir 30: 13689-13698, 2014.

21. Akkari ACS, Papini JZB, Garcia GK, Franco MKKD, Cavalcanti LP, Gasperini A, Alkschbirs MI, Yokaichyia F, de Paula E, Tófoli GR and de Araujo DR: Poloxamer 407/188 binary thermosensitive hydrogels as delivery systems for infiltrative local anesthesia: Physico-chemical characterization and pharmacological evaluation. Mater Sci Eng C Mater Biol Appl 68: 299-307, 2016.

22. Dumortier G, Grossiord JL, Agnely F and Chaumeil JC: A review of poloxamer 407 pharmaceutical and pharmacological characteristics. Pharm Res 23: 2709-2728, 2006.

23. Santos Akkari AC, Ramos Campos EV, Keppler AF, Fraceto LF, de Paula E, Tófoli GR and de Araujo DR: Budesonide-hydroxypropyl-β-cyclodextrin inclusion complex in binary poloxamer 407/403 system for ulcerative colitis treatment: A physico-chemical study from micelles to hydrogels. Colloids Surf B Biointerfaces 138: 138-147, 2016.

24. Mello JC, Moraes VW, Watashi CM, da Silva DC, Cavalcanti LP, Franco MK, Yokaichiya F, de Araujo DR and Rodrigues T: Enhancement of chlorpromazine antitumor activity by Pluronics F127/L81 nanostructured system against human multidrug resistant leukemia. Pharmacol Res 111: 102-112, 2016.

25. Nascimento MHM, Franco MKKD, Yokaichyia F, de Paula E, Lombello CB and de Araujo DR: Hyaluronic acid in Pluronic F-127/F-108 hydrogels for postoperative pain in arthroplasties: Influence on physico-chemical properties and structural requirements for sustained drug-release. Int J Biol Macromol 111: 1245-1254, 2018.

26. Valero M and Dreiss CA: Modulating Pluronics micellar rupture with cyclodextrins and drugs: Effect of pH and temperature. J Phys Conf Ser 549: 012010, 2014.

27. Mills CM and Marks R: Side effects of topical glucocorticoids. Curr Probl Dermatol 21: 122-131, 1993.

28. FDA Post market Drug Safety: http://www.fda.gov/Drugs/DrugSafety/PostmarketDrugSafetyInformationforPatientsandProviders/ucm107845.htm

29. Kohno S, Endo H, Hashimoto A, Hayashi I, Murakami Y, Kitasato H, Kojima F, Kawai S and Kondo H: Inhibition of skin sclerosis by 15deoxy delta12,14-prostaglandin J2 and retrovirally transfected prostaglandin D synthase in a mouse model of bleomycin-induced scleroderma. Biomed Pharmacother 60: 18-25, 2006.

30. Kon K, Ikejima K, Hirose M, Yoshikawa M, Enomoto N, Kitamura T, Takei Y and Sato N: Pioglitazone prevents early-phase hepatic fibrogenesis caused by carbon tetrachloride. Biochem Biophys Res Commun 291: 55-61, 2002.

31. Ghosh AK, Bhattacharyya S, Lakos G, Chen SJ, Mori Y and Varga J: Disruption of transforming growth factor beta signaling and profibrotic responses in normal skin fibroblasts by peroxisome proliferator-activated receptor gamma. Arthritis Rheum 50: 1305-1318, 2004.

32. Mantel A, Newsome A, Thekkudan T, Frazier R and Katdare M: The role of aldo-keto reductase 1C3 (AKR1C3)-mediated prostaglandin D2 (PGD2) metabolism in keloids. Exp Dermatol 25: 38-43, 2016.

33. Arai I, Takano N, Hashimoto Y, Futaki N, Sugimoto M, Takahashi N, Inoue T and Nakaike S: Prostanoid DP1 receptor agonist inhibits the pruritic activity in NC/Nga mice with atopic dermatitis. Eur J Pharmacol 505: 229-235, 2004.

34. Farnesi-de-Assunção TS, Alves CF, Carregaro V, de Oliveira JR, da Silva CA, Cheraim AB, Cunha FQ and Napimoga MH: PPAR-γ agonists, mainly 15d-PGJ(2), reduce eosinophil recruitment following allergen challenge. Cell Immunol 273: 23-29, 2012.

35. Fujimura Y, Tachibana H and Yamada K: Peroxisome proliferator-activated receptor ligands negatively regulate the expression of the high-affinity IgE receptor Fc epsilon RI in human basophilic KU812 cells. Biochem Biophys Res Commun 297: 193-201, 2002.

36. Miyazaki Y, Tachibana H and Yamada K: Inhibitory effect of peroxisome proliferator-activated receptor-gamma ligands on the expression of IgE heavy chain germline transcripts in the human B cell line DND39. Biochem Biophys Res Commun 295: 547-552, 2002.

37. Klotz L, Burgdorf S, Dani I, Saijo K, Flossdorf J, Hucke S, Alferink J, Nowak N, Beyer M, Mayer G, et al: The nuclear receptor PPAR gamma selectively inhibits Th17 differentiation in a T cell-intrinsic fashion and suppresses CNS autoimmunity. J Exp Med 206: 2079-2089, 2009.

38. Vieira SM, Cunha TM, França RF, Pinto LG, Talbot J, Turato WM, Lemos HP, Lima JB, Verri WA Jr, Almeida SC, et al: Joint NOD2/RIPK2 signaling regulates IL-17 axis and contributes to the development of experimental arthritis. J Immunol 188: 5116-5122, 2012.

39. Toda M, Leung DY, Molet S, Boguniewicz M, Taha R, Christodoulopoulos P, Fukuda T, Elias JA and Hamid QA: Polarized in vivo expression of IL-11 and IL-17 between acute and chronic skin lesions. J Allergy Clin Immunol 111: 875-881, 2003.

40. Koga C, Kabashima K, Shiraishi N, Kobayashi M and Tokura Y: Possible pathogenic role of Th17 cells for atopic dermatitis. J Invest Dermatol 128: 2625-2630, 2008.

41. Di Cesare A, Di Meglio P and Nestle FO: A role for Th17 cells in the immunopathogenesis of atopic dermatitis? J Invest Dermatol 128: 2569-2571, 2008.

42. Theoharides TC, Alysandratos KD, Angelidou A, Delivanis DA, Sismanopoulos N, Zhang B, Asadi S, Vasiadi M, Weng Z, Miniati A and Kalogeromitros D: Mast cells and inflammation. Biochim Biophys Acta 1822: 21-33, 2012.

43. Heo WI, Lee KE, Hong JY, Kim MN, Oh MS, Kim YS, Kim KW, Kim KE and Sohn MH: The role of interleukin-17 in mouse models of atopic dermatitis and contact dermatitis. Clin Exp Dermatol 40: 665-671, 2015.

44. Batista DI, Perez L, Orfali RL, Zaniboni MC, Samorano LP, Pereira NV, Sotto MN, Ishizaki AS, Oliveira LM, Sato MN and Aoki V: Profile of skin barrier proteins (filaggrin, claudins 1 and 4) and Th1/Th2/Th17 cytokines in adults with atopic dermatitis. J Eur Acad Dermatol Venereol 29: 1091-1095, 2015.

45. Coutinho DS, Anjos-Valotta EA, do Nascimento CVMF, Pires ALA, Napimoga MH, Carvalho VF, Torres RC, E Silva PMR and Martins MA: 15-Deoxy-delta-12,14-prostaglandin J2 inhibits lung inflammation and remodeling in distinct murine models of asthma. Front Immunol 8: 740, 2017.